

Direct Single Point Diamond Cutting of Stavax Assisted with Ultrasonic Vibration to Produce Optical Quality Surface Finish

X. D. Liu, X. Ding, L. C. Lee, F. Z. Fang and G. C. Lim
Singapore Institute of Manufacturing Technology, Singapore

1. Introduction

Steel is widely used in the plastic molding industry. However, it is well known that steel cannot be machined using diamond tools due to the excessive tool wear, which is mainly caused by diamond graphitization [1-4]. In vacuum, diamond is converted to graphite when the environmental temperature is over 1800°K. If iron elements are present, the conversion temperature is reduced to between 400°K and 600°K. To minimize diamond graphitization when machining steel, various approaches have been attempted. High carbon steels were cut in a carbon rich environment (methane and ethyne) [4, 5]. It was found that a carbon rich environment helped to reduce the diamond tool wear rate. Evans [6] observed that the tool wear was much reduced when the cutting area was cooled using cryogenic method. Ultrasonic vibration assisted machining has been used for cutting, grinding, and tapping by Kumabe since 1960s. He suggested that steel could be machined using diamond tool by applying ultrasonic vibration [7]. However, it was only recently that ultrasonic vibration assisted machining has been successfully used in ultra-precision machining. Moriwaki and Shamoto [8] developed an ultrasonic vibration assisted cutting (USC) system to cut steel to mirror surface finish. The tool life was also increased significantly. Klocke and Rubenach [9] built a similar device and used it to make steel parts for industrial applications.

This paper reports on the use of a USC system for theoretical and experimental studies of the lubrication of the tool-chip interface.

2. Experimental Set-Up

The experiments were conducted on a Precitech ultra-precision lathe (Optimum 4200). A mixture of compressed air and baby oil was used as the lubricant. The work material was Stavax with a hardness of HRC 40 to 45 (stainless steel, AISI 420, 0.38% C, 0.9% Si, 0.5 Mn, 13.6% Cr, 0.3% V). It is widely used as molding tools on account of its high strength, corrosion resistance and machinability.

An ultrasonic vibration system was constructed as shown in Fig. 1. The ultrasonic vibration unit was mounted on a height-adjusting frame with a clamping ring. One clamp position is at the static node of the vibration wave. To compensate for the poor rigidity with only one static clamp point, a dynamic clamp point was introduced at the free end of the horn. This will strengthen the rigidity in the thrust direction. The arrangement would largely eliminate the lateral vibration. The effect on the longitude vibration is minimal. The diamond tool was mounted at the end of horn and vibrated in the direction of the horn axis -the cutting direction- with a frequency of 40 kHz. The vibration amplitude was adjustable from 2 to 24 μm .

A precision non-contact capacity ADE Microsense gauging system was used to measure the amplitude of the ultrasonic vibration. The vibration signals were analyzed by Fast Fourier Transform (FFT). The machined surface roughness was measured using a Wyko white light interferometer.

3. Lubrication during Ultrasonic Vibration Assisted Cutting

For each vibration amplitude, the cutting speed has to be properly selected to achieve mirror surface finish. Researchers have suggested that the cutting speed need to be only below the maximum vibration speed. Our investigation showed that the practical cutting speed to achieve mirror surface finish

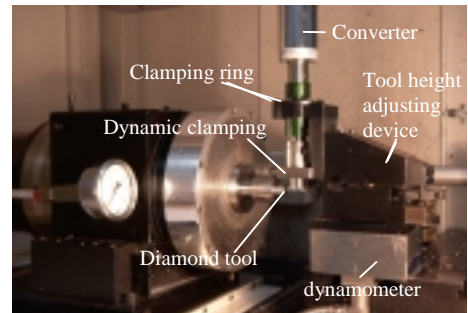


Fig.1 Ultrasonic vibration assisted cutting system

can be significantly lower than the maximum vibration speed. To understand this, an analysis of the tool-chip gap and the lubrication at the cutting zone was undertaken.

During ultrasonic vibration assisted cutting, the workpiece moves towards the cutting tool, with the cutting tool vibrating at a frequency f and amplitude A , as shown in Fig. 2. When the diamond tool is in the retraction part of the vibration cycle, the vibrating speed increases rapidly. Once the speed is higher than the cutting speed, v , the tool rake face starts to separate from the chip, say, at point a . The gap between the tool and chip, Δd , increases as the tool retracts further. Once the tool has passed the neutral point, the vibration speed slows down. When it is again equal to the cutting speed on the other half of the cycle, the gap reaches its largest value at point c . As the vibration speed slows down, the gap, Δd , decreases from the maximum value to zero at point b . The tool vibration motion can be express with the formula:

$$y = A \sin \omega t \quad (1)$$

where $\omega = 2\pi f$, and t is time.

The gap between the tool and chip is given by:

$$\Delta d = A(\sin \omega t_a - \sin \omega t) - v(t - t_a) \quad t_a < t < t_b \quad (2)$$

where t_a and t_b are t at point a and b , respectively.

After the differentiation of equation (2) with respect to t , and simplifying, the times for equal speeds at a and b is:

$$t = \frac{1}{\omega} \cos^{-1} \left(\frac{v}{2A\pi f} \right) \quad (3)$$

The maximum gap can be calculated with equation (2) once t_a and t_b are found. Fig. 3 shows the variation of the maximum gaps between the tool and the chip with the cutting speed at different vibration amplitudes. The maximum gap is found to decrease almost linearly with an increase in the cutting speed. When the cutting speed is very low, the maximum gap is around twice the value of the vibration amplitude. When the cutting speed reaches the maximum vibration speed, no gap exists between the tool and the chip.

To simplify the analysis of the lubrication mechanism at the tool-chip interface, some assumptions can be made. As the tool nose radius (1mm) is much larger than the depth of cut (6 μm), the tool contact arc is considered to be a straight line. Hence, $OABC$ is the contact area between the tool and the chip (see Fig. 4). OA is the tool-chip contact length. It is further assumed that the coolant fluid enters the gap only from the side AB , and no coolant enters from CB or OA , since AB is much longer than CB and OA . There is also no coolant coming from OC , which is the cutting edge.

When the rake face retracts from the chip by dz , the coolant advances by $dl \sin \kappa$ towards the cutting edge, in the negative y direction. The volume of the vacuum created should be equal to the volume filled in by the coolant; that is:

$$l_o a_c dz = l a_c dz + a_c h dl \quad (4)$$

$$(l_o - l) a_c v_s dt \sin \kappa = a_c h u_f dt \quad (5)$$

$$\frac{u_f}{\sin \kappa (\ln h)} = l_o - l \quad (6)$$

where κ is the cutting edge angle; l_o is the tool-chip contact

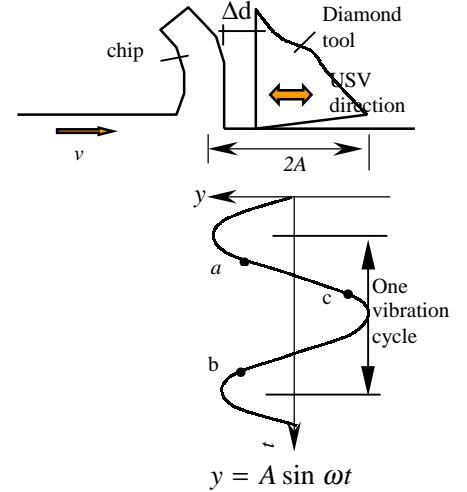


Fig. 2 Ultrasonic vibrating of diamond tool

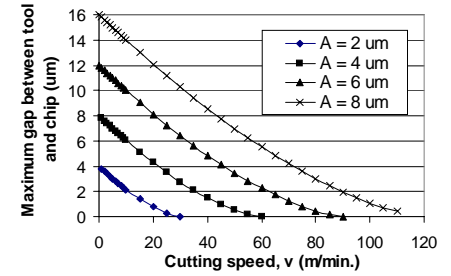


Fig. 3 Maximum gaps between tool-chip vs cutting speed

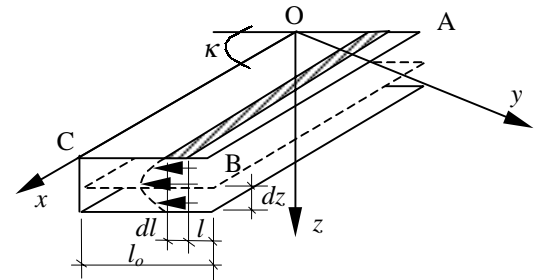


Fig. 4 Model for coolant filling into tool-chip

length; l is the distance advanced by the coolant at time t ; a_c is the depth of cut; h is the gap between the tool and the chip at time t ; v_s is the separation speed of the tool from the chip ($= h'$); and u_f is the average speed of the lubricant moving front at l .

To eliminate the variate l , differentiate equation (6) with respect to time t , and simplify it. Hence:

$$u_f = C_1 \frac{h'}{h^{1-\sin \kappa}} = C_1 \frac{-A\omega \sin \omega t - v}{(A(\sin \omega t_a - \sin \omega t) - v(t - t_a))^{1-\sin \kappa}} \quad (7)$$

To determine the value of the lubricant advancement over time t , the above equation is integrated:

$$l = Ch^{\sin \kappa} = C(A(\sin \omega t_a - \sin \omega t) - v(t - t_a))^{\sin \kappa} \quad (8)$$

where C is a constant. From equations (7) and (8), it is observed that in initial stage, the lubricant moves very fast and then slows down.

4. Results and Discussion

Theoretically, using equation (8) it is able to determine whether the lubricant fully fills the tool-chip gap and lubricates the tool rake face by comparing the calculated l and the tool-chip contact length, l_o . However, the presence of the constant C in equation (8) limits its direct application to predict the coolant filling condition. From experiments, it was found that when the cutting speed was 5 m/min and the vibration amplitude 2 μm , depth of cut 6 μm and feedrate of 10 $\mu\text{m}/\text{rev}$, a machined surface finish of 8 nm Ra can be achieved (see Fig. 5). This shows that the coolant has reached the cutting edge and fully lubricated the tool. The maximum gap computed using equation (2) is about 3 μm . This condition can be used as the criterion to study the coolant filling effect under the same conditions except for the cutting speed and the vibration amplitude. The following equation can be used for the comparison:

$$R_o = l/l_o = \left(\frac{(A(\sin \omega t_a - \sin \omega t) - v(t - t_a))^{\sin \kappa}}{3} \right) \quad (9)$$

where l_o is the tool-chip contact length for the cutting conditions mentioned above. If R_o is larger than 1, the corresponding cutting speed is considered as the critical value. Fig. 6 shows the calculated critical cutting speed at which the tool-chip gap is fully filled for a given vibration amplitude. It can be seen that the critical cutting speed increases almost linearly with an increase in the vibration amplitude.

In the experiments it was difficult to ascertain whether the tool-chip gap was fully filled by direct observation. Instead, the finish of chip underside was used to judge the effect of lubrication. If there were no tear marks on the machined surface (see Fig. 7(a)), the tool was considered to be well lubricated and cooled. Based on this, the experimental critical cutting speed was obtained and plotted in Fig. 5. It can be seen that when the vibration amplitude is below 5 μm , the calculated results are in good agreement with the experimental values. However, for high cutting speeds the differences can be quite large. This is because equation (9) only considers the filling condition of the coolant, but does not take into account the heat which it is being conducted away. In high cutting speed, the cutting temperature at the cutting region can be very high. If the coolant does not stay long enough between the tool and the chip and insufficient heat is conducted away, this results in work material adhering to the cutting edge and results in a poorer surface roughness. Furthermore, the high temperature accelerates the diamond graphitization and exacerbates the tool wear. The prevalence of material adhesion can be conveniently deduced by examining the underside of the chips. At low cutting speeds the cooling time was sufficient and the underside of the chips were found to be very smooth (see

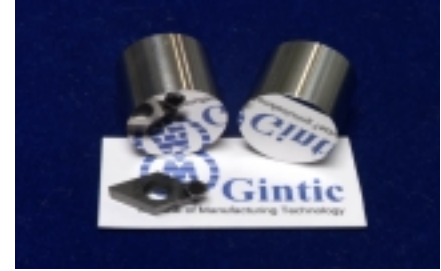


Fig. 5 Machined steel parts with mirror finish

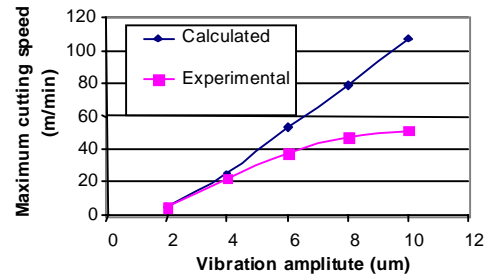


Fig. 6 Maximum cutting speed for a given vibration amplitude

Fig. 7(a)). This implies that there is little or no work material adhesion problem. On the other hand, grooves and tear marks could be clearly seen on the underside of the chips at high cutting speeds (see Fig. 7(b)). This suggested that material adhesion occurred at these cutting conditions. The lubricant was unable to reach to the cutting edge or, there was insufficient cooling time.

From the above analysis, it appears that increasing the amplitude while maintaining the same cutting speed can improve the lubricating and cooling effects. However, large vibration amplitude generates more heat at transducer connections and this can damage the vibration transducer through overheating. Therefore, low vibration amplitude ($<4\ \mu\text{m}$) and low cutting speeds ($< 20\ \text{m/min}$) are usually preferred.

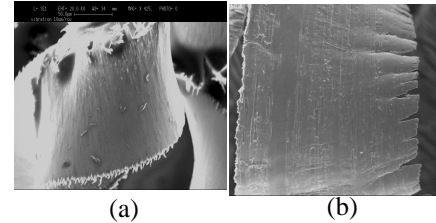


Fig. 7 chip underside with (a) sufficient cooling (b) insufficient cooling

5. Conclusions

From the above study, some conclusions can be drawn:

- An ultrasonic vibration assisted cutting system using a static and a dynamic clamping points provides an adequate stiffness in the lateral direction.
- The maximum gap between the tool and the chip decreases almost linearly with an increase in the cutting speed.
- The coolant filling speed is much faster at the early stage than the later stage of the vibration cycle.
- The calculated and experimental critical cutting speeds were found to be in good agreement at low vibration amplitudes. However, large differences existed at high vibration amplitudes due to the prevalence of work material adhesion on the cutting edge.

6. Reference

- [1] Komanduri R. and Shaw M.C., *Wear of Synthetic Diamond when Grinding Ferrous Metals*, Nature, 1975, v255, pp 211-213.
- [2] Brooks C. A., *The Friction of Diamond at Elevated Temperatures and Its Interfacial Reactions with Steel*, Industrial Diamond Review, 1971, v31, pp 21-24.
- [3] Tanaka T., Ikawa N. and Tsuaw H., *Affinity of Diamond for Metals*, Annals of the CIRP, 1981, v30, No.1, pp 241-245.
- [4] Hitchiner M. P. and Wilks J., *Some Remarks on the Chemical Wear of Diamond and Cubic BN during Turning and Grinding*, Wear, 1987, v114, pp 327-338.
- [5] Casstevens J., *Diamond Turning of steel in carbon saturated atmospheres*, Precision Engineering, v5, No. 1, 1983, pp 9-15
- [6] Evans C., *Cryogenic diamond turning of stainless steel*, Annals of the CIRP, 1991, v40, No.1, pp 571-573
- [7] Kumabe J., *Vibration Cutting*, Jikkyou Publishing Co., Tokyo, 1979.
- [8] Moriwaki T. and Shamoto E., *Ultraprecision Diamond Turning of Stainless Steel by Applying Ultrasonic Vibration*, CIRP, v40, No. 1, 1991, pp 559-562
- [9] Klocke F., and Rubenach O., *Ultrasonic Assisted Diamond Turning of Steel and Glass*, Proceedings of the International Seminar on Precision Engineering and Micro Technology, Aachen, Germany, July 2000, pp 179-189.

Acknowledgements: The authors would like to thank Stephen Wan, Wu Hu, Ng Seow Tong and Shaw Kah Chuan for their contributions to the work associated with the paper.